25-29 August 2024
inter.noise
NANTES FRANCE

Weight minimization of train floors with acoustical and structural constraints

Ulf Orrenius[1]
Akustikdoktorn Sweden AB
Drakens Gränd 6 II
111 30 Stockholm, Sweden

Johan Wittsten[2]
AWER Geoteknik AB
Södra Långgatan 2
392 32 Kalmar

ABSTRACT

For high-speed trains, high noise levels are generated in the bogie from wheel-rail contact and aero-acoustic sources. Manufacturers try to minimize the floor transmission to the interior, e.g. by applying damping layers or by other measures. For vehicle noise control measures, the goal is often to achieve the sound reduction needed at lowest possible mass. Here, an optimization scheme is applied to minimize the mass of an extruded floor panel. Constraints are defined by limiting the maximum local floor deflection from passenger loads according to EN 12663-1 and the A-weighted interior sound level.

Recognizing the periodic nature of the floor structure, a Finite Element model of a single periodic cell is set up, using periodic boundary conditions and the floor sound reduction is determined using a Statistical Energy Analysis approach. An analytic beam model is applied to determine the floor deflection from the passenger load. Design solutions meeting the constraints with the smallest possible mass are sought. Starting with a floor structure with 23.3 kg/m², a final design with 18.0 kg/m2 is reached. In addition, the transmitted sound through the floor is reduced by 8 dBA. Convergence from different starting points is verified.

1. BACKGROUND

1.1 Rail carbodies in aluminium

Aluminium carbodies, although more expensive than corresponding steel designs, can be made lighter and to a high degree of pressure tightness, features which makes them the primary candidates for high-speed trains. For such carbodies, wall, roof and floor structures are normally made from extruded hollow profiles that are welded together, cf. Figure 1.

As sound pressure levels below the carbody can be well above 120 dB(A), very effective sound barriers are needed for train floors, e.g. above bogies and diesel engines, as well as for the roof below pantographs of high-speed trains. For high-speed trains the leading bogies are particularly exposed to aero-acoustic sound generation. An overview of railway sources, and

[1] ulf@akustikdoktorn.se

Part of the numerical work presented was undertaken when both authors were working for Bombarier Transportation Sweden Sweden AB.

[2] johan@awer.se.

the challenges associated with sound transmission of structures made of extruded profiles, is given in [1].

Figure 1: Structural layout of extruded body-shell section.

Due to their poor acoustic insulation properties, train structures made in extruded profiles, are subject to extensive noise control treatments and there is a strong interest from the industry to optimize such designs using computer models. The principal application is to support decision-making in the design process, preferably in its early stages when the design still can be influenced without major cost and project time losses. For this reason, models should be able to correctly resolve the effects of design alterations that have an impact on both noise transmission, including dedicated noise control treatments such as introduction of damping layers, and structural strength satisfying the structural requirement. In addition, such models should be able to predict sound transmission properties for realistic excitation representations in the entire audio frequency range.

1.2 Topology optimization

Topology optimization as a method for reducing weight has a long and successful history with products for which low weight is essential for their performance and life cycle costs, like aircraft and aerospace structures, and more recently also for electric cars and high-speed ships and boats utilizing hydrofoil technology. For rail structures the methodologies are less applied, although case studies can be found in references [2], [3] and in [4]. In terms of life cycle costs, light-weight railcars offer clear advantages, in particular regarding rail and wheel wear [5] and energy consumption [6]. In addition, axle load limits, as defined in e.g. TSI C (2008) 648 [7], may restrict the load carrying capacity of rail cars below the potential, unless the carbody weight is kept low.

Although the noise insulation is a key performance indicator of floor and roof structures, Multidisciplinary Design Optimization (MDO) studies, for which acoustic performance is part of the definition of the design space, are scarce. One reason is the lack of methodology for accurate and computationally efficient calculation of acoustic insulation of carbody structures in the full audio range.

1.3 Functional requirements on rail carbodies

The main functions of a rail vehicle carbody are to provide passengers with sufficient comfort and safety. To achieve these two main functions, the carbody must provide a number of lower-level functions, e.g. strength, sound reduction and fire safety. For these functions, it is often possible to define requirements which must be fulfilled to design and manufacture a vehicle. Accordingly, the structural design of car-bodies is driven by a large number of functional requirements. Examples of such requirements are compliance with structural load cases according to EN 12663-1 [8]. This standard includes, but is not limit ed to, couper loads, passengers load, lifting load cases and requirements on equipment attachments. In the

standard, also lower bounds for natural frequencies are indirectly given (which in turn affects the ride comfort). Additional requirements also apply, which are not only governed by the structural design, such as, noise reduction capacity [9], pressure tightness, resistance to fire and thermal insulation. On top of all this, the structure must comply with weight and production cost restrictions.

Ideally, for a practically useful MDO, all relevant design parameters need to be expressed mathematically and included in the MDO formulation. For rail structures, structural optimization work is reported with respect to carbody structural strength in reference [4] and for the fatigue life of carbody components life in reference [10]. Although requirements for high acoustic insulation is clearly a driver of increased carbody mass, the inclusion of noise insulation requirements is not common in the MDO literature. In references [6] and [9] mass minimization of a rail car inner floor structure and a load carrying sandwich body panel respectively, are addressed, both with structural and acoustic constraints. In reference [11], a weight minimization approach of an extruded floor structure with acoustic constraints is presented, but without accounting for static loads and associated constraints.

In the present work, an MDO approach is applied for which the passenger load carrying capacity of a train floor in line with EN 12663-1 [8] is used to define its required flexural stiffness. The acoustic insulation is indirectly represented by the A-weighted sound pressure in an interior cavity, subject to the acoustic loading of a diffuse field below the train floor.

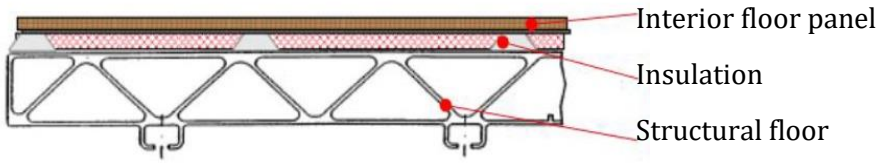

Figure 2: Typical lay-up of a train floor including interior floor panel and insulation.

In Figure 2, a lay-up drawing of a complete floor is displayed. Clearly, the addition of an interior floor panel and relevant acoustic insulation, will improve the floor sound reduction, as well as its thermal insulation, but the strategy here is to design a structural floor with a sufficiently high sound insulation, to form a basis for the sound insulation of the complete floor including acoustic package. By using the mass of the structural floor effectively, less mass needs to be added in sound reducing measures.

2. AIM

The overall objective is to define and apply a practically useful algorithm for mass minimization of train floors made in extruded profiles, with the required sound transmission and static strength as constraints. The algorithm is based on robust calculation methods for sound insulation and floor strength with respect to passenger load.

3. MODELLING STRATEGY

3.1 Periodic theory for acoustic modelling.

Traditionally, methodologies for industrial acoustic predictions are based on either Statistical Energy Analysis (SEA) or Finite Elements (FE), sometimes combined with Boundary Elements (BE). For large structures at audio frequencies, the fluid-structure FE-BEM models become numerically expensive whereas statistical models are not detailed enough for parametric studies.

For periodic engineering structures, a practically useful concept is to determine the parameters needed for an SEA model from the solution of a small FE model. This FE model is then built up from one or a few cells of the periodic structure and periodic boundary conditions are applied. The FE model can be kept small and computationally efficient, allowing for

parametric studies of the effect of design changes. This concept has been applied for train structures in [13], [14] and [16], and for aircraft structures in [14], [15] and [18]. In reference [17] the concept is applied to minimize the weight of an extruded train floor, subject to acoustical and structural constraints.

In the present work the periodic theory developed by Langley et al for two-dimensional structures [20] is applied. Consider a general structure with 2D periodicity. A periodic cell can be extracted from the structure and modeled using the Finite Element method. The degrees of freedom **q** of the cell can be partitioned into interior (*I*), edge (*L, R, B, T*) and corner (*LB, RB, LT, RT)* degrees of freedoms. The internal degrees of freedom are not connected to other periodic cells. The vibration response of the structure at a given frequency can be analyzed by specifying a phase lag between the displacement degrees of freedom at the left, right, bottom and top edges,

$$\mathbf{q}_R = \mathrm{e}^{-\mathrm{i}\varepsilon_x}\,\mathbf{q}_L, \quad \mathbf{q}_T = \mathrm{e}^{-\mathrm{i}\varepsilon_y}\,\mathbf{q}_B. \tag{1}$$

Similar transformations apply to the corner degrees of freedoms. The terms ε_x and ε_y are referred to as 'phase constants'. For free wave propagation in an undamped structure these constants are real and can take values between $-\pi$ and π.

To apply periodic boundary conditions, it is necessary to ensure that the node locations on opposite edges and corners of the cell are identical. The complete vector of local degrees of freedom of the cell can be ordered so that $\mathrm{q} = [\mathbf{q}_I\ \mathbf{q}_B\ \mathbf{q}_T\ \mathbf{q}_L\ \mathbf{q}_R\ \mathbf{q}_{LB}\ \mathbf{q}_{LB}\ \mathbf{q}_{LT}\ \mathbf{q}_{RT}]^{\mathrm{T}}$. The undamped harmonic equation of motion for the unit cell is then given by $[\mathbf{K}-\omega^2\mathbf{M}]\mathbf{q} = \mathbf{F}$, where **M** and **K** are the mass and stiffness matrices for the cell and **F** is the generalized force vector. An eigenvalue problem can be derived from this that can be phrased in different ways depending on whether frequency is fixed, or phase constants epsilon is fixed. This enables that also frequency dependent materials can be modeled accurately.

By solving the algebraic eigenvalue problem, the properties of the free waves propagating in the periodic structure are obtained. From these properties, the vibro-acoustic properties of the structure are calculated using the concepts of the 'wave approach to SEA' [21] Expressions are derived for the modal density, damping loss factor, and distribution of squared velocity response per unit energy of the structure. Using a Fourier transform approach, the resonant radiation efficiency, resonant and non-resonant transmission losses, and acoustic input power are also obtained. See reference [20] and [22] for details.

3.2 **Acoustic transmission model**

For the purposes of the floor optimization, consider a transmission model with one interior receiving cavity, the saloon cavity, and one exterior sending cavity, the bogie cavity. The cavities are separated by the train floor with area S taken as $3\times3\ m^2$. The saloon cavity is taken to be parallelepipedal with dimensions $3 \times 3 \times 2.5\ m^3$, for which all surface areas are assumed to have an absorption coefficient of $\alpha = 0.28$ resulting in an equivalent absorption area $A = \sum_{i=1}^{6} S_i\alpha_i = 12.7\ m^2 S$. Assuming the sound field in the saloon cavity being diffuse and the result of sound transmission though the floor only, the sound pressure level in the saloon cavity in frequency band i, is given by,

$$L_{p,saloon,i} = L_{p,bogie,i} - R_i + 10\log_{10}\frac{S}{A}, \tag{2}$$

in which $L_{p,bogie,i}$ is the bogie cavity sound pressure level of frequency band i, R_i the sound reduction index of the floor of frequency band I whereas $\mathrm{A}' = \mathrm{A}/(1-\alpha)$. To represent $L_{p,bogie}$, a sound level spectrum measured in the motor bogie cavity for a train at 90 km/h is applied.

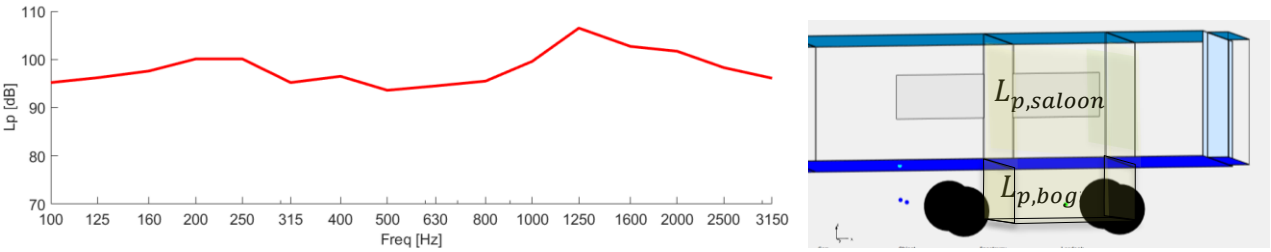

Figure 3: Measured sound pressure level spectrum in a train bogie.

For the transmission model, the periodic subsystem implementation within the VA1 software is used, see Section 3.1 above and reference [18]. Hereby, the extruded floor panel sound reduction index R_i can accurately be determined [16].

3.3 **Static deflection model**

The floor was assumed to carry a distributed load of 500 kg/m^2, representative to the passenger load of a fully loaded metro car, which may be more than needed for high-speed cars. The floor was represented by a simply supported beam with unity width to calculate the deflection of the floor center line, which was approximated as,

$$\delta = \frac{5qL^4}{384EI}, \tag{3}$$

where, q is the distributed load, L is the beam length, E is Young's modulus, and I' is the beam area moment of inertia. The material properties of the floor design are stated in Table 1.

Table 1. Material properties of the structural floor

Sub-panel thickness [mm]	Young's modulus [GPa]	Density [kg/m^3]	Damping loss factor
2.8	72	2700	0.02

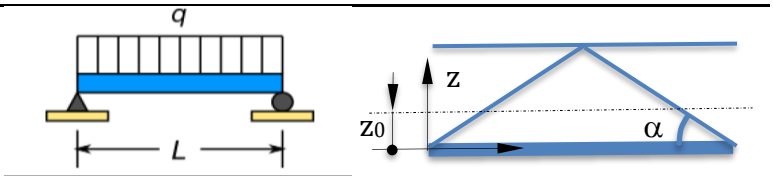

Figure 4: Freely supported beam with a distributed load (left) and cell geometry details (right).

For an asymmetric beam with thin-walled elements, the moment of inertia around the neutral layer is calculated as,

$$I'_{y,tot} = I'_{y,upper} + I'_{y,lower} + \bar{I}'_{y,inner} \tag{4}$$

$$I'_{y,upper} = \frac{t_{upper}^3}{12} + t_{upper}(L_z - z_0)^2\,,\; I'_{y,lower} = \frac{t_{lower}^3}{12} + t_{lower}{z_0}^2 \tag{5}$$

$$\bar{I}'_{y,inner} = \frac{L_z t_{inner}}{\sin\alpha}\left[\frac{{L_z}^2}{3} - L_z z_0 + {z_0}^2\right], \tag{6}$$

where the neutral layer is at (see Figure 4),

$$\bar{z}_0 = L_z \cdot \frac{2t_{upper}+t_{inner}}{2(t_{upper}+t_{lower}+t_{inner})}. \tag{7}$$

Cell geometry details are illustrated in Figure 4 and in Figure 5. Note that $I'_{y,inner}$ and z_0 are locally depending on the x-coordinate, but for practical purposes using the spatial averages $\bar{I}'_{y,inner} = \frac{2}{L_x}\int_0^{L_x/2} I'_{y,inner} dx$ and $\bar{z}_0 = \frac{2}{L_x}\int_0^{L_x/2} z_0 dx$ is sufficient.

For the calculation of center line deflection, free boundaries are assumed. Generally speaking, the flexural stiffness of the carbody walls will add rotational stiffness at the floor edges, meaning that the assumption of free edges leads to a conservative estimate of the floor deflection.

4. TRAIN FLOOR OPTIMIZATION

A mass minimization problem of the 3 × 3 m² floor structure is defined, combining structural and acoustic constraints in the optimization process. The objective function is taken to be the mass per unit area *m* of the structural floor. No inner floor was considered.

The structural floor must be strong enough to hold the passenger load and in addition provide enough sound insulation against noise transmitted from the bogie cavity. The A-weighted sound level in the saloon cavity $L_{p,saloon}$, is taken as acoustical constraint and the center line floor deflection under distributed load δ, is used as mechanical constraint. Design parameters were sub-panel thicknesses (t_{upper}, t_{inner}, t_{lower}) and cell size variables (L_x, L_z).

4.1 Constructing the floor optimization model

An FE model of a typical extruded floor was previously used with the periodic cell concept [14], [16] to determine acoustic transmission properties; see Section 3.1 for a description of the underlying theory. To increase calculation speed, the original FE model is here reduced in size to include only a single 0.19 × 0.3 m² structural cell. The train floor section is then assembled from 15 × 10 periodically replicated cells oriented in the *xy*-plane.

Even though the original geometry is more complex, the assumption here is that topological optimization of the simpler cell geometry model is useful for design guidance.

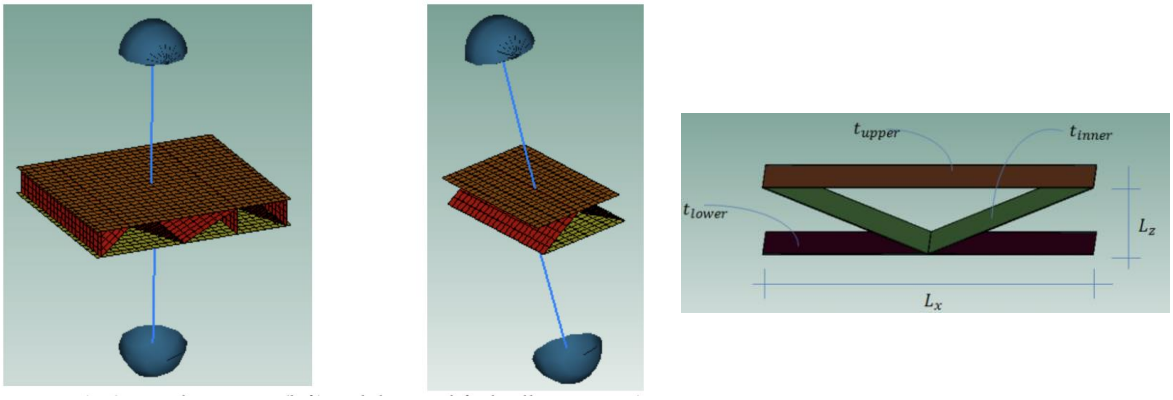

Figure 5. Original structure (left) and the simplified unit cell geometry (center) with geometric parameters indicated (right).

A design space is defined by setting lower and upper bounds of the sub-panel thicknesses and unit cell size, as described in Table 2.

Table 2. Upper and lower bounds of the geometry parameters applied in the optimization.

Parameter [mm]	L_x	L_z	t_{inner}	t_{upper}	t_{lower}
Lower bound	50	20	1	1	1
Upper bound	300	60	5	5	5

The panel mass per unit area is determined from the total mass of all sub-panels in the cell divided by the cell area.

4.2 **Constraints**

The optimization routine was set up with constraints to reflect the design targets. The maximum deflection of the floor center line δ was kept "as is", e.g. that of the original floor, whereas the saloon sound level $L_{pA,saloon}$ was required to be reduced by 8 dB, reflecting the desired sound insulation of the floor. The data are given in Table 3.

Table 3. Centerline deflection and interior sound level of the original and the target structure

	δ [mm]	$L_{p,saloon}$ $[dBA]$
Original structure	17.6	86
Target structure	17.6	78

The A-weighted sound level in the saloon was formed as $L_{pA,saloon} = \sum_{i=1}^{N} 10^{L_{A\ saloon,i}/10}$ In which $L_{A\ saloon,i}$ are the one third octave band components of the A-weighted saloon spectrum. Based on the frequency content of the bogie cavity spectrum, the frequency range included was taken as 100-3150 Hz.

4.3 **Optimization algorithm**

Calculation of the cost function and the deflection constraint was performed in MATLAB®, which is also used to call VA-One to calculate the sound reduction index of the floor structure using the periodic cell module (PCM). For the iterative updating of design variables, the built-in *fmincon* function is used, operating with the Sequential Quadratric Programming algorithm. Below is a listing of the sequence of steps taken at every iteration:

(1) MATLAB sets new parameter values based on the outputs of the *fmincon* routine.
(2) MATLAB starts and operates VA-One in the background.
(3) VA-One creates a new FE model with the updated cell geometry.
(4) The updated FE model is meshed, and the mass is calculated.
(5) The PCM is called to replicate the cell geometry over the xy-plane onto a larger area and calculates the transmission loss.
(6) MATLAB closes VA-One
(7) MATLAB calculates δ, the deflection of the structural floor.
(8) MATLAB uses the sound reduction index from the PCM to calculate $L_{A,saloon}$, the A-weighted sound level in the saloon cavity.
(9) MATLAB compares δ and $L_{A,saloon}$, with the constraints specified.

Each iteration involves several different sub-processes (3)-(8), in which computation is made with new parameter values. In step (1) *fmincon* is used to find the gradient of the objective function to determine the parameter vector for the next iteration. If the constraints are not met in step (9), the algorithm changes the parameters and updates the geometry to make a new calculation to iteratively find a set of design variables for which both constraints are met. When both constraints are met, the optimizer continues to change the parameters to reduce surface mass while respecting the constraints. As the optimizer runs this iterative process, the parameter values converge into a final design, as illustrated by Figure 6. Starting from the original panel design, convergence is reached typically within 15 iterations.

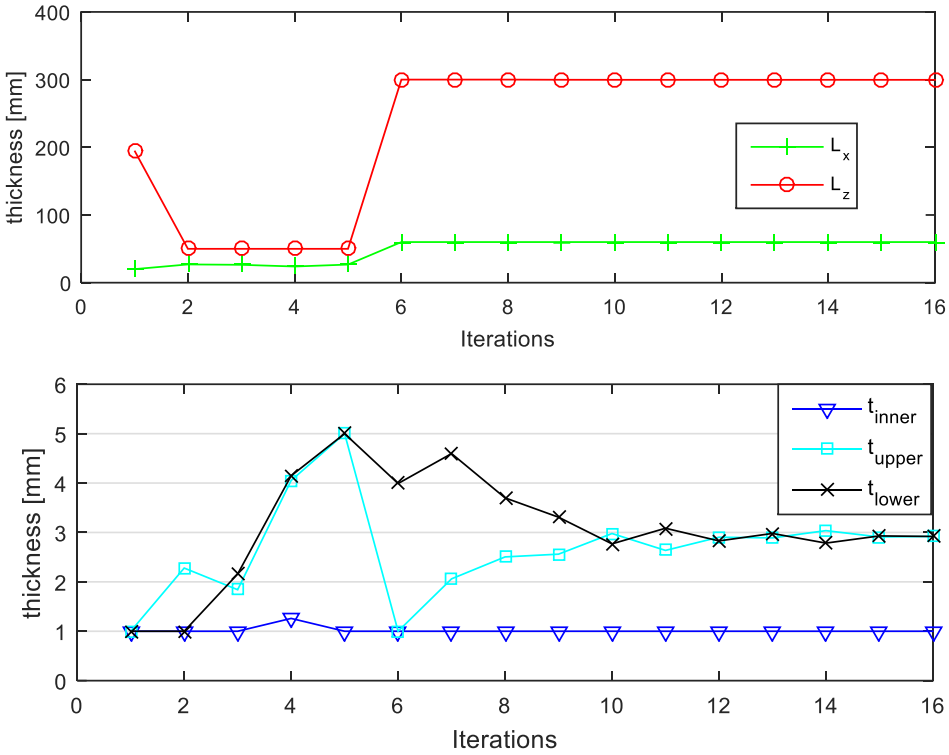

Figure 6: Geometry parameter development during the iterations when starting from the lower parameter bounds.

4.4 **Convergence test**

Figure 7 shows the development of surface mass of two optimization runs when setting the starting point at either (A) the original design or (B), the lower parameter bounds as defined in Table 2. The final surface mass is the same for both runs.

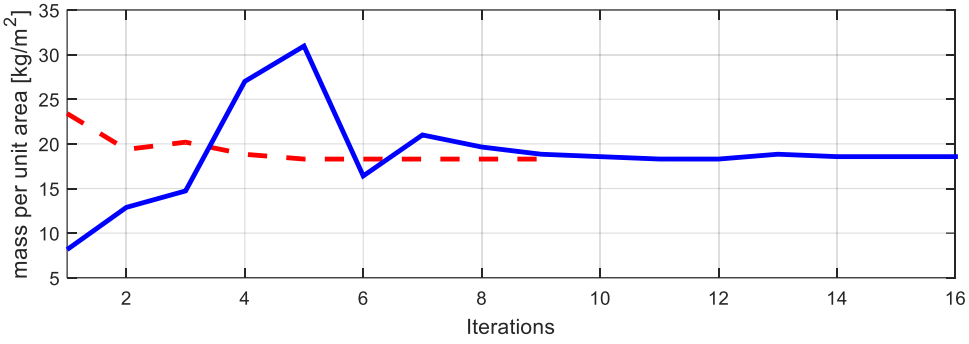

Figure 7: Mass density development for iterations from two different starting points.

5. RESULTS

5.1 **Floor parameters**

The properties of the original and final floor designs are given in Table 4.

Table 4. Properties of the original and final design.

[mm]	L_x	L_z	t_{inner}	t_{upper}	t_{lower}	m [kg/m²]
original	190	57.5	2.8	2.8	2.8	23.3
final	300	60	1	2.8	2.8	18.0
asymmetric	300	60	1	1	4.6	18.0

In addition, parameters of an asymmetric design are given, with the lower sub-panel much thicker than the upper one. It has been found that such designs are greatly beneficial with respect to sound reduction.

5.2 **Transmission loss results**

To better understand how the sound reduction depends on the geometry of the sub-panels, four different topologies were evaluated using the periodic cell method: (i) original structure, (ii) optimized structure, (iii) asymmetric, (iv) asymmetric flipped upside-down.

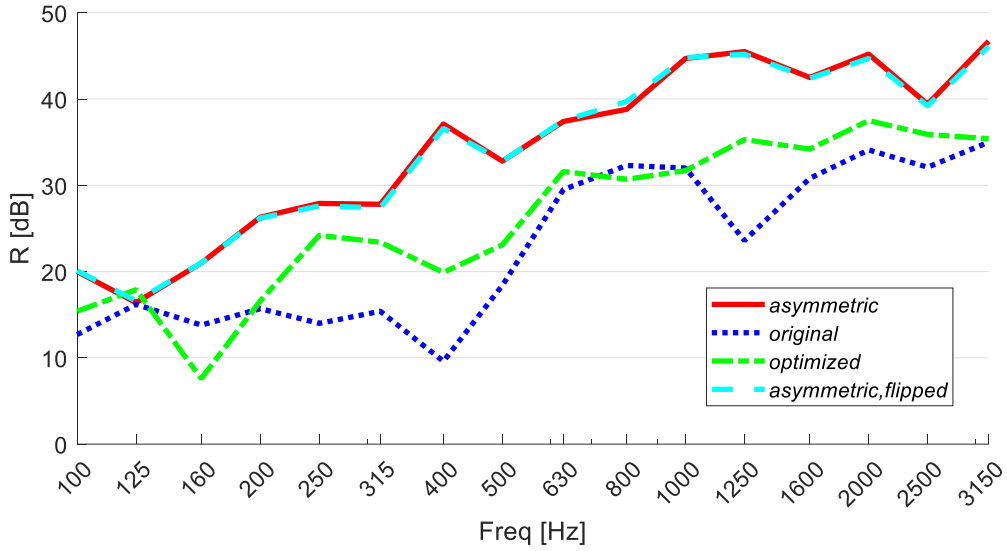

Figure 8: Calculated sound reduction indices for different designs as defined in Table 4.

The results displayed in Figure 8 show that the optimized design has significantly improved sound reduction properties in relation to the original design. One reason is that the increased distance between the web intersections, L_x, shifts the cut-on frequency of the local sub-panel modes to lower frequencies, see reference [16] for details.

It is notable that the sound reduction of the optimized design is significantly improved at 1250 Hz compared to the original design, which is the frequency band with the highest input noise levels. Apparently, the optimization routine favors design solutions that succeed in suppressing the peak level of the incoming sound.

Moreover, the asymmetric design further improves the sound reduction at the same surface mass as the optimized design. The "price" is that the floor is less stiff, with about 50% higher deflection δ than the original design.

6. DISCUSSION

6.1 **Problem formulation**.

Structural topology optimization is a powerful design tool but its successful application for industrial problems requires a well thought-out plan that takes into consideration a high number of factors. The definition of the design domain is fundamental including manufacturing restrictions etc.

In spite of the large number of functional requirements governing the carbody design as described in Section 1.3, only two constraints were included in the present MDO formulation, In addition, the design space was restricted by the bounds set for the design parameters as of Table 2. These limits on the sub-panel thicknesses shall be viewed as a first attempt to account for manufacturing requirement regarding extruded profiles.

The selection of using a deflection constraint for the floor is based on the authors engineering judgement that of the load cases described in EN 12663-1, the one corresponding to passenger load most directly affects the floor geometry. Moreover, it can easily be written in a mathematical form, which may be more difficult for e.g., requirements on carbody resistance to buckling at high coupler loads or at impact loads associated with roll-over accident [8]. In an engineering design process involving floor optimization, it is required that any novel floor designs are integrated within a complete carbody model and validated with respect to the "safety driven" load cases, see e.g. reference [4].

6.2 Sound reduction performance of the floor

It is not intuitively obvious why the asymmetric floor design is so much better in terms of sound reduction than the original symmetric design. The radiation efficiency of a radiating panel is defined as,

$$\sigma = \frac{W_{rad}}{\overline{v^2}\rho_0 c_0 S}, \tag{8}$$

with S being the panel surface, W_{rad} the power radiated, $\sqrt{\overline{v^2}}$ the spatial average of the panel RMS velocity and $\rho_0 c_0$ is the specific acoustic impedance of air. In the below graph, sound radiation efficiencies are plotted for the original and the asymmetric structure, calculated using the PCM implementation within VA One. Also, radiation efficiencies of the asymmetric and original designs when turned upside down are displayed.

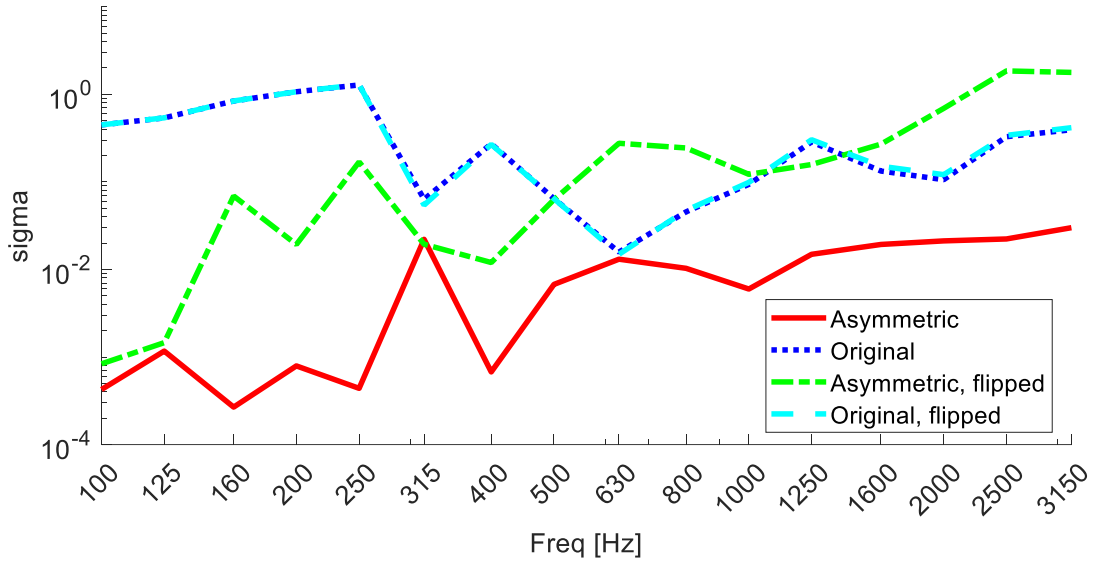

Figure 9: Sound radiation efficiencies for different geometry designs as defined in Table 4.

Clearly, the asymmetric design radiates much less sound than the original design at a given vibration velocity level. By reducing the thickness of the upper (thinner) sub-panel, and also increasing L_x, the cut-on frequency for the local sub-panel modes is shifted to substantially lower frequencies, significantly decreasing the panel's fluid structure coupling.; see reference [16]. In addition, the coincidence frequency for the upper sub-panel is shifted to higher frequencies. Both these frequency shifts contribute to reduced radiation and accordingly reduced sound transmission as of Figure 9.

6.3 Outlook

The present problem set-up should be viewed as a pilot study illustrating how acoustic performance can be included in a MDO approach for periodic, load carrying structures. To reduce modelling complexity, while keeping the problem formulation such that the results still

have practical interest, only two functional constraints were considered: panel sound reduction and static deflection due to a distributed passenger load.

For future work, it is recommended to review the static and dynamic load cases of the EN 12663-1 in more detail, and potentially include a more detailed description of the structural load cases acting on the floor. Optional to the deflection constraints used here, limits on material stress can be imposed, or in combination with the static deflection and local deformation. This could be done with a FE model of the structural floor.

In the present work the constraints were defined in relation to the reference floor deflection and sound transmission. If optimization is used for a commercial product, the constraints should preferably be set in absolute rather than in relative terms. This ultimately requires knowledge in what is a possible allowed deflection, under a specified load, if deflection should be used as a constraint.

Similarly, the design space should be defined such that upper and lower design variable bounds directly correspond to practical limitation for production purposes. For the asymmetric design analyzed, thin plates thickness could be problematic regarding the extrusion process or when welding or point loads.

Although not part of the load carrying structure, inner floors should be added in a more complete optimization scheme addressing acoustic performance, e.g. as being made in reference [16]. Furthermore, an attractive alternative formulation to the mass minimization problem addressed, is to minimize the sound pressure with mass and deflection constraints.

In summary, before implementing novel floor extrusion geometries in rail carbodies, design candidates need to be validated by more complete simulation and testing schemes, partly because other load cases than those addressed here need to be checked and partly because extruded floor structures are generally not fully periodic, as illustrated in Figure 5.

7. CONCLUSION

The results show that it is possible to combine structural and acoustic constraints to support the design of a train floor structure in extruded profiles. and the optimization algorithm applied could effectively solve the mass minimization problem at hand. Starting with a floor structure with mass per unit area of 23.3 kg/m^2 as reference, the algorithm converged into a final design with 18.0 kg/m^2. Also, the final design is a much better sound barrier than the original one with transmitted A-weighted sound level reduced by 8 dB. In addition, an asymmetric floor design is shown to significantly improve the sound reduction at the cost of reduced stiffness.

Before implementing novel floor extrusion geometries in rail carbodies, they need to be validated by more complete simulation and testing schemes.

8. ACKNOWLEDGEMENTS

The authors would like to thank Torsten Kohrs at Alstom Germany for checking the manuscript and Per Wennhage at KTH, Stockholm and Rabah Hadjit at ESI USA, for support regarding the optimization process. The authors are also grateful to ESI for making the VA One software available for the project.

.

REFERENCES

[1] Thompson, D., *Railway Noise and Vibration: Mechanisms, Modelling and Means of Control*, Elsevier, Oxford, 2008.

[2] Lang, D., Radford, D.W. Design Optimization of a Composite Rail Vehicle Anchor Bracket. *Urban Rail Transit* **7**, 84–100 (2021).

[3] Cascino, A. et al., Dynamic size optimization approach to support railway carbody lightweight design process. *Proceedings of the Institution of Mechanical Engineers, Part F: Journal of Rail and Rapid Transit. 2023;237(7):871-881*.

[4] M. Takagaki et al, Design of Carbody by Method of Structural Optimization, *QR of RTRI, Vol 59, No 1, 2018.*

[5] Wennberg, D., et al, Benefits of Weight Reduction in High-Speed Train Operations., *ZEV rail Glasers Annalen, ISSN 1618-8330, vol. 137, no3, pp. 77-87, March 2013*

[6] Wennberg, D. (2013). Multi-Functional Composite Design Concepts for Rail Vehicle Car Bodies (PhD dissertation, KTH Royal Institute of Technology).

[7] 2008/232/EC: Commission Decision of 21 February 2008 concerning a technical specification for interoperability relating to the rolling stock sub-system of the trans-European high-speed rail system (notified under document number C(2008) 648).

[8] EN 12663-1:2010+A1:2014 Railway applications - Structural requirements of railway vehicle bodies - Part 1: Locomotives and passenger rolling stock (and alternative method for freight wagons).

[9] Cameron, C. J., et al (2014). On the balancing of structural and acoustic performance of a sandwich panel based on topology, property, and size optimization., *Journal of Sound and Vibration, 333(13), 2677–2698.*

[10] Miao, B.R. et al., Multidisciplinary design optimization of lightweight carbody for fatigue assessment. *Materials and Design, Volume 194, 2020, 108910.*

[11] D. Yao, et al, Lightweight design and sound insulation characteristic optimisation of railway floating floor structures, *Applied Acoustics, Volume 156, 2019, Pages 66-77,*

[12] Li, H. et al., A modelling approach for noise transmission through extruded panels in railway vehicles, *Journal of Sound Vibration, vol. 502, 2021.*

[13] Orrenius, U. et al., Analysis of sound transmission through periodic structures typical of railway carbodies and air-craft fuselages, *Proceedings NOVEM 2009, Oxford, England.*

[14] Orrenius, U. et al., Wave modelling in predictive acoustics: Application to rail-vehicles and aircraft, J*. of Wave motion, 51 (2014), pp. 635-649.*

[15] Orrenius, U., et al., Analysis of sound transmission through aircraft fuselages excited by turbulent boundary layer or diffuse acoustic pressure fields, *Proc. Internoise 2009, Ottawa.*

[16] Orrenius, U. and Kohrs, T. 2022, Modelling of train floor sound transmission using coupled FE-SEA analysis. *Proceedings Internoise 2022, Glasgow.*

[17] Wittsten, J., 2016, Optimization of Train Floors with Acoustic and Structural Constraints, *MSc thesis, Chalmers University of Technology, BOMX02-16-6.*

[18] Cotoni, V., Langley, R.S. and Shorter, Vibro-acoustic analysis of aircraft fuselage panels using a periodic SEA subsystem formulation, *Proceedings of Noise-Con 2008, Dearborn, MI, USA, July 2008*.

[19] VA One 2023a, User's Guide, ESI, 2023.

[20] Cotoni, V. et al., A statistical energy analysis subsystem formulation using finite element and periodic structure theory, *Journal of Sound and Vibration 318 (2008) 1077–1108.*

[21] Lyon, R.H., DeJong, R.G., *Theory and Application of Statistical Energy Analysis*, second ed., Butterworth-Heinemann, Boston, 1995.

[22] Langley, R.S., A note on the force boundary conditions for two-dimensional periodic structures with corner freedoms, *Journal of Sound and Vibration 167 (1993), p. 377-381.*